HHS Public Access

Author manuscript

J Am Chem Soc. Author manuscript; available in PMC 2023 September 14.

Published in final edited form as:

J Am Chem Soc. 2022 September 14; 144(36): 16303–16309. doi:10.1021/jacs.2c07489.

Copper Hydride-Catalyzed Enantioselective Olefin Hydromethylation

Yuyang Dong,
Department of Chemistry, Massachusetts Institute of Technology, Cambridge, Massachusetts 02139, United States

Kwangmin Shin,
Department of Chemistry, Massachusetts Institute of Technology, Cambridge, Massachusetts 02139, United States

Binh Khanh Mai,
Department of Chemistry, University of Pittsburgh, Pittsburgh, Pennsylvania 15260, United States

Peng Liu,
Department of Chemistry, University of Pittsburgh, Pittsburgh, Pennsylvania 15260, United States

Stephen L. Buchwald
Department of Chemistry, Massachusetts Institute of Technology, Cambridge, Massachusetts 02139, United States

Abstract

The enantioselective installation of a methyl group onto a small molecule can result in the significant modification of its biological properties. While hydroalkylation of olefins represents an attractive approach to introduce alkyl substituents, asymmetric hydromethylation protocols are often hampered by the incompatibility of highly reactive methylating reagents and a lack of general applicability. Herein, we report an asymmetric olefin hydromethylation protocol enabled by CuH catalysis. This approach leverages methyl tosylate as a methyl source compatible with the reducing base–containing reaction environment, while a catalytic amount of iodide ion transforms the methyl tosylate *in situ* into the active reactant, methyl iodide, to promote the hydromethylation. This method tolerates a wide range of functional groups, heterocycles, and pharmaceutically relevant frameworks. Density functional theory studies suggest that after the stereoselective hydrocupration, the methylation step is stereoretentive, taking place through an S_N2–type oxidative addition mechanism with methyl iodide followed by a reductive elimination.

Corresponding Authors pengliu@pitt.edu.
Present Address: Department of Chemistry, Sungkyunkwan University, Suwon 16419, Republic of Korea

Supporting Information

The Supporting Information is available free of charge at https://pubs.acs.org/doi/10.1021/jacs.2c07489.
Experimental procedures and characterization data for all new compounds, including NMR spectra, SFC traces, computational details, and Cartesian coordinates of all computed structures (PDF)

The authors declare no competing financial interest.

The introduction of a methyl group, despite its small size and simplicity, can induce profound changes in the properties of a molecule.[1–4] In biologically active compounds, the incorporation of a methyl group may result in conformational changes which increase the structural complementarity of a lead compound to its target receptor with minimal impact on its molecular weight and lipophilicity (Figure 1A).[5–7] While common approaches for the introduction of other single-carbon fragments rely on the asymmetric functionalization of olefins,[8–13] few strategies have been reported for the direct installation of methyl groups. Standard methods to directly install methyl groups rely on conjugate additions to polarized olefins using preformed organometallic reagents facilitated by chiral Lewis acid catalysts.[14–17]

Hydromethylation is an attractive approach for the introduction of a methyl group to an olefin. Even though not enantioselective, some notable methods to hydromethylate olefins include Kambe's Zr–catalyzed reductive coupling protocol[18] and Tilley's Sc-catalyzed methane C–H activation process.[19] Additionally, Baran has developed a formal olefin hydromethylation protocol, utilizing Fe-catalyzed H-atom transfer and a formaldehyde hydrazone as the methyl surrogate.[20] The reaction demonstrated a high degree of functional group tolerance and was used in the late-stage functionalization and isotopic labeling of complex molecules. More recently, Shenvi disclosed a hydroalkylation protocol utilizing Ni/Mn dual catalysis, in which MeI and CD_3I were utilized to afford the corresponding methylated products,[21] and Nocera has reported on the use of photochemically generated Me-radical from acetic acid.[22] Finally, Frederich delineated the use of a superstoichiometric quantity of Tebbe's reagent.[23] Despite the emergence of several formal hydromethylation strategies, controlling the absolute stereochemistry at the newly formed C–Me bond remains a largely elusive goal (Figure 1B).[18–24] The most relevant asymmetric variant is limited to Lu and Fu's elegant Co-catalyzed hydromethylation of fluoroalkenes (Figure 1C).[25]

Our group and others have leveraged CuH-catalysis to forge C–C bonds in a variety of enantioselective transformations,[26] including intramolecular hydroalkylation,[27] intermolecular allylation,[28] and 1,2-carbonyl addition.[29–36] These reactions utilize an *in situ* generated enantioenriched Cu-alkyl species to engage various electrophiles. We sought to employ a CuH-catalyst system in combination with an appropriate electrophilic methyl source to effect the enantioselective hydromethylation of olefins (Figure 1D).[37,38] Due to the highly reactive nature of common electrophilic methyl sources, such as methyl iodide,[39,40] we anticipated the major challenge to be the incompatibility between the methylating reagents and reducing reaction conditions and/or the base necessary for CuH generation or regeneration. Therefore, we chose to employ a less reactive methyl source, methyl tosylate (MeOTs).[41]

We commenced our investigation by examining the hydromethylation of a styrene allylic ether (**1a**), employing MeOTs as the methyl source. Utilizing several bidentate chiral bisphosphine ligands (**L1–L5**) in combination with CuOAc, the olefin hydromethylation product **2a** was formed in moderate yield and low er (entries 1–5, Table 1). We identified (*S*)–DTBM–SEGPHOS (**L5**) as the optimal ligand, among those we tested, for this transformation (entry 5). Examining various copper(l) halides (entries 6–8) revealed that the use of CuI provides the desired product in excellent yield and with a very high level

of enantioselectivity. To simplify the reaction protocol, a precatalyst (**L5**)CuI (**P1**) was prepared and utilized in subsequent experiments. The use of **P1** afforded **2a** in similar yield and selectivity to that obtained using a mixture of Cul and **L5** (entry 9).

The improved reaction outcome with the use of CuI prompted further investigation into the role of iodide ion.[42,43] A series of experiments were carried out by systematically varying the equivalents of iodide ion in the presence of a constant amount of copper (6 mol % Cu; entry 10: 12 mol % I^-; entry 11: 9 mol % I^-; entry 12: 4.5 mol % I^-; entry 13: 3 mol % I^-; entry 14: 1.5 mol % I^-; see Supporting Information, Table S2). We observed that increasing the iodide ion concentration concomitantly led to increased enantioselectivity of **2a** and decreased conversion of **1a** (entry 10). We hypothesized that the *in situ* formation of methyl iodide (MeI)[42,43] facilitates the asymmetric hydromethylation through a proposed catalytic cycle shown in Scheme 1. Enantioselective hydrocupration of **1a** with ligated CuH species (**3**) generates the Cu-alkyl intermediate (**4**). Catalytic quantities of I^- convert MeOTs to the more reactive MeI,[44] which undergoes methylation with **4** to form product **2a**. The resulting ligated CuI intermediate regenerates **3** through sequential Cu–alkoxide generation and σ-bond metathesis with $PhMe_2SiH$. Two competing processes take place concurrently: (1) the epimerization of **4**,[45] and (2) the trapping of MeI by NaOTMS. With a higher iodide ion concentration, the more rapid methylation of **4** with Mel leads to the observed increase in enantioselectivity. At the same time, higher iodide ion concentrations increase the rate of MeOTMS formation, leading to the observed decrease in conversion. In a similar way, lowering the effective concentration of Mel increases the steady-state concentration of **4**, which facilitates the productive methylation while minimizing trapping of the methylating reagent (see Supporting Information for detail, Scheme S1). Taken together, modulating the iodide ion concentration offers an operationally simple handle to tune the enantioselectivity or yield of this reaction.

Density functional theory (DFT) calculations were carried out to corroborate our proposed hydromethylation catalytic cycle, namely the participation of *in situ* formed Mel and the apparent iodide effect. The calculations were performed at the M06/6–311+G(d,p)-SDD(Cu, I)/SMD(THF)//B3LYP-D3/6–31G(d)-SDD(Cu, I) level of theory using **1a** as the model substrate with **L5**-supported Cu catalyst (Figure 2; see Supporting Information for Computational Details). The hydrocupration of **1a** with CuH catalyst **3** through **TS-1** was found to be exergonic and kinetically facile, preferentially giving (*R*)-Cu-alkyl intermediate **4**. The hydrocupration TS leading to (*S*)-Cu-alkyl intermediate **4′** (via **TS-1′**) is 7.7 kcal/mol higher in energy than **TS-1**, due to the substituents of the alkene being placed in quadrants occupied by the C_2-symmetric ligand **L5**, leading to unfavorable steric repulsions (see Supporting Information, Figure S3).[46]

From Cu-alkyl intermediate 4, we first assessed the reactivity of MeI toward methylation through an S_N2-type oxidative addition[47–49] via **TS-2A** ($\Delta G^{\ddagger}$ = 18.7 kcal/mol with respect to **4**; see Supporting Information, Figure S4 for 3D TS structures). The resulting cationic species **5** undergoes rapid stereoretentive reductive elimination (via **TS-3**) to furnish **2a**,[47] which is consistent with the absolute configuration of the hydromethylation products (*vide infra*). The activation barrier for the methylation using MeOTs as the methylating reagent via **TS-2D** is 12.8 kcal/mol higher in energy than **TS-2A**, suggesting that MeI

is indeed the active form of the methylating reagent and the higher reactivity of MeI is critical to suppressing benzylcopper epimerization[45] and thus achieving higher product enantioselectivity.[50]

Several alternative methylation mechanisms involving MeI were also considered. Methylation through the direct S_N2 nucleophilic substitution via **TS-2B** (see Figure S5 for 3D TS structures),[48,49] involving simultaneous formation of the C–C bond and the dissociation of the C–I and Cu–C bonds, requires a 6.4 kcal/mol higher barrier than **TS-2A**. This indicates that this stereoinvertive pathway is less favorable than the stereoretentive pathway via **TS-2A** and **TS-3**. The concerted oxidative addition via a three-centered transition state **TS-2C** is 18.2 kcal/mol less favorable. Finally, the outer-sphere concerted dissociative electron transfer (DET) mechanism[51,52] was also ruled out due to the high activation barrier ($\Delta G^{\ddagger}_{sol}$ = 22.8 kcal/mol with respect to **4**) calculated using the modified Marcus theory (see SI for details).[53,54] Collectively, these computational results corroborated our proposed catalytic cycle and provided insight into the mechanism by which the critical C–CH_3 bond is formed.

We then used our mechanistic understanding of the olefin hydromethylation protocol to aid our exploration for substrates amenable to this transformation (Table 2). Given our understanding of the role of iodide ions in this reaction, we first optimized reaction conditions by modulating the loading of **P1** and/or adding substoichiometric quantities of MeI. For instance, in the case of olefins that delivered good yields in the presence of **P1** alone, substoichiometric MeI was added to increase the enantioselectivity of the transformation (**2g** and **2l**). For substrates that exhibited low conversions under the standard reaction conditions, decreasing the amount of **P1**, thereby reducing the effective iodide ion concentration, led to an increased product yield at the expense of enantioselectivity (*vide supra*, **2h–k, 2n**). Additionally, slow addition of MeOTs was demonstrated to be a viable method to increase the product yield (**2d** and **2f**). The reaction proceeded effectively with substrates bearing both electron-donating and -withdrawing functional groups. A range of heterocycles were also well-tolerated, such as indazole (**2c**), pyrrole (**2d**), benzoxazole (**2e**), piperazine (**2f**), pyrrolidine (**2g**), furan (**2g**), indole (**2h**), thiophene (**2l**), oxazole (**2m**), morpholine (**2p**), and phenothiazine (**2p**). Several pharmaceuticals were derivatized to further demonstrate the functional group compatibility of this protocol, including from antihistamine Cinnarizine (**2f**), respiratory stimulant Ethamivan (**2k**), nonsteroidal anti-inflammatory Oxaprozin (**2m**), and anti-infective Naftifine (**2n**). To access **2m** in high yield, NaOTMS was slowly introduced to the reaction mixture to prevent deprotonation at the α-carbon of the ester. The absolute configuration of the products was determined by comparing the optical rotation of **2b**, **2d**, and **2i** to literature values.[55–57]

To further highlight the synthetic utility of the asymmetric olefin hydromethylation protocol, the synthesis of **2k** was carried out on a 5.0 mmol scale, resulting in improved yield and comparable enantioselectivity to the 0.5 mmol scale reaction (Scheme 2A). To showcase the utility of our method, we devised a three-step asymmetric synthetic sequence to **8a**, a substrate which binds the σ_1-receptor (Scheme 2B).[58] Starting from commodity chemical 2-bromo-6-methoxynaphthalene (**8b**), a Pd-catalyzed Heck reaction between **8b** and 1,1-diethoxyethene furnished the α,β-unsaturated aldehyde **8c** in high yield. Subsequent

reductive amination (**8d**) followed by CuH-catalyzed hydromethylation furnished **8a** in high enantiomeric purity (95:5 er) and 27% yield over three steps. The general substructure of **8a** is widely present in a range of pharmaceutical lead compounds.[59–66]

In summary, we have developed a CuH-catalyzed enantioselective olefin hydromethylation protocol. This method is tolerant of a wide range of functional groups and heterocycles. This method was also used for the derivatization of several pharmaceuticals, and in a concise three-step asymmetric synthesis of a σ_1-receptor binding molecule. Mechanistic evidence suggests a crucial role of catalytic iodide ion in effecting both the yield and enantioselectivity of the asymmetric methylation. Density functional theory calculations revealed that the methylation occurs through an S_N2-type oxidative addition giving a formal Cu(III) intermediate, which undergoes reductive elimination to furnish the methylated product.

Supplementary Material

Refer to Web version on PubMed Central for supplementary material.

ACKNOWLEDGMENTS

Research reported in this publication was supported by the National Institutes of Health (R35-GM122483 and R35GM128779). We thank the National Institutes of Health for a supplemental grant for the purchase of supercritical fluid chromatography (SFC) equipment (GM058160-17S1). We thank Nippon Chemical Industrial Co., Ltd. for the generous donation of (*S*,*S*)-QuinoxP* ligand. DFT calculations were carried out at the Center for Research Computing at the University of Pittsburgh, the Extreme Science and Engineering Discovery Environment (XSEDE) supported by the National Science Foundation Grant Number ACI-1548562. We are grateful to Drs. Simon Rössler, Michael Strauss, Alexander Schuppe, Sheng Feng, Dennis Kutateladze, and Christine Nguyen (MIT) for advice on the preparation of this manuscript.

REFERENCES

(1). Barreiro EJ; Kummerle AE; Fraga CAM The Methylation Effect in Medicinal Chemistry. Chem. Rev 2011, 111, 5215–5246. [PubMed: 21631125]

(2). Chen P; Fatayer S; Schuler B; Metz JN; Gross L; Yao N; Zhang Y. The Role of Methyl Groups in the Early Stage of Thermal Polymerization of Polycyclic Aromatic Hydrocarbons Revealed by Molecular Imaging. Energy Fuels 2021, 35, 2224–2233. [PubMed: 33574639]

(3). Xia H; Tang Y; Zhang Y; Ni F; Qiu Y; Huang C-W; Wu C-C; Yang C. Highly efficient blue electroluminescence based on TADF emitters with spiroacridine donors: methyl group effect on photophysical properties. J. Mater. Chem. C 2022, 10, 4614–4619.

(4). Rao J; Liu X; Li X; Yang L; Zhao L; Wang S; Ding J; Wang L. Bridging Small Molecules to Conjugated Polymers: Efficient Thermally Activated Delayed Fluorescence with a Methyl-Substituted Phenylene Linker. Angew. Chem., Int. Ed 2020, 59, 1320–1326.

(5). Schönherr H; Cernak T. Profound Methyl Effects in Drug Discovery and a Call for New C–H Methylation Reactions. Angew. Chem, Int. Ed 2013, 52, 12256–12267.

(6). Sun S; Fu J. Methyl–containing pharmaceuticals: Methylation in drug design. Bioorg. Med. Chem. Lett 2018, 28, 3283–3289. [PubMed: 30243589]

(7). Leung CS; Leung SSF; Tirado–Rives J; Jorgensen WL Methyl Effects on Protein–Ligand Binding. J. Med. Chem 2012, 55, 4489–4500. [PubMed: 22500930]

(8). Franke R; Selent D; Börner A. Applied Hydroformylation. Chem. Rev 2012, 112, 5675–5732. [PubMed: 22937803]

(9). Ebner C; Carreira EM Cyclopropanation Strategies in Recent Total Syntheses. Chem. Rev 2017, 117, 11651–11679.

(10). Cometti G; Chiusoli GP Asymmetric induction in carbonmethoxylation of vinylaromatics. J. Organomet. Chem 1982, 236, 31–32.

(11). Konrad TM; Fuentes JA; Slawin AMZ; Clarke ML Highly Enantioselective Hydroxycarbonylation and Alkoxycarbonylation of Alkenes using Dipalladium Complexes as Precatalysts. Angew. Chem, Int. Ed 2010, 49, 9197–9200.

(12). Deng Y; Wang H; Sun Y; Wang X. Principles and Applications of Enantioselective Hydroformylation of Terminal Disubstituted Alkenes. ACS Catal. 2015, 5, 6828–6837.

(13). Brezny AC; Landis CR Recent Developments in the Scope, Practicality, and Mechanistic Understanding of Enantioselective Hydroformylation. Acc. Chem. Res 2018, 51, 2344–2354. [PubMed: 30118203]

(14). Hioe J; Zipse H. Radical stability and its role in synthesis and catalysis. Org. Biomol. Chem 2010, 8, 3609–3617. [PubMed: 20544076]

(15). López F; Minnaard AJ; Feringa BL Catalytic Enantioselective Conjugate Addition with Grignard Reagents. Acc. Chem. Res 2007, 40, 179–188. [PubMed: 17370989]

(16). Alexakis A; Bäckvall JE; Krause N; Pàmies O; Diéguez M. Enantioselective Copper-Catalyzed Conjugate Addition and Allylic Substitution Reactions. Chem. Rev 2008, 108, 2796–2823. [PubMed: 18671436]

(17). Pichon D; Morvan J; Crévisy C; Mauduit M. Copper-catalyzed enantioselective conjugate addition of organometallic reagents to challenging Michael acceptors. Beilstein J. Org. Chem 2020, 16, 212–232. [PubMed: 32180841]

(18). Terao J; Watanabe T; Saito K; Kambe N; Sonoda N. Zirconocene-catalyzed alkylation of aryl alkenes with alkyl tosylates, sulfates and bromides. Tetrahedron Lett. 1998, 39, 9201–9204.

(19). Fontaine F-G; Tilley TD Control of Selectivity in the Hydromethylation of Olefins via Ligand Modification in Scandocene Catalysts. Organometallics 2005, 24, 4340–4342.

(20). Dao HT; Li C; Michaudel Q; Maxwell BD; Baran PS Hydromethylation of Unactivated Olefins. J. Am. Chem. Soc 2015, 137, 8046–8049. [PubMed: 26088401]

(21). Green SA; Huffman TR; McCourt RO; van der Puyl V; Shenvi RA Hydroalkylation of Olefins To Form Quaternary Carbons. J. Am. Chem. Soc 2019, 141, 7709–7714. [PubMed: 31030508]

(22). Zhu Q; Nocera DG Photocatalytic Hydromethylation and Hydroalkylation of Olefins Enabled by Titanium Dioxide Mediated Decarboxylation. J. Am. Chem. Soc 2020, 142, 17913–17918.

(23). Law JA; Bartfield NM; Frederich JH Site-Specific Alkene Hydromethylation via Protonolysis of Titanacyclobutanes. Angew. Chem., Int. Ed 2021, 60, 14360–14364.

(24). Parnes ZN; Bolestova GI; Akhrem IS; Vol'pin ME; Kursanov DN Alkyl groups migration from tetra-alkyl-silanes, -germanes, and -stannanes to carbenium ions, effected by Lewis acids: a novel method for synthesising hydrocarbons with a quaternary carbon atom. J. Chem. Soc., Chem. Commun 1980, 748–748.

(25). Li Y; Nie W; Chang Z; Wang J–W; Lu X; Fu Y. Cobalt-catalysed enantioselective C(sp3)–C(sp3) coupling. Nat. Catal 2021, 4, 901–911.

(26). Liu RY; Buchwald SL CuH-Catalyzed Olefin Functionalization: From Hydroamination to Carbonyl Addition. Acc. Chem. Res 2020, 53, 1229–1243. [PubMed: 32401530]

(27). Wang Y-M; Bruno NC; Placeres ÁL; Zhu S; Buchwald SL Enantioselective Synthesis of Carbo- and Heterocycles through a CuH-Catalyzed Hydroalkylation Approach. J. Am. Chem. Soc 2015, 137, 10524–10527.

(28). Wang Y-M; Buchwald SL Enantioselective CuH-Catalyzed Hydroallylation of Vinylarenes. J. Am. Chem. Soc 2016, 138, 5024–5027. [PubMed: 27042864]

(29). Dong Y; Schuppe AW; Mai BK; Liu P; Buchwald SL Confronting the Challenging Asymmetric Carbonyl 1,2-Addition Using Vinyl Heteroarene Pronucleophiles: Ligand–Controlled Regiodivergent Processes through a Dearomatized Allyl–Cu Species. J. Am. Chem. Soc 2022, 144, 5985–5995. [PubMed: 35341240]

(30). Meng F; Jang H; Jung B; Hoveyda AH Cu-Catalyzed Chemoselective Preparation of 2-(Pinacolato)boron-Substituted Allylcopper Complexes and their In Situ Site-, Diastereo-, and Enantioselective Additions to Aldehydes and Ketones. Angew. Chem., Int. Ed 2013, 52, 5046–5051.

(31). Meng F; Haeffner F; Hoveyda AH Diastereo- and Enantioselective Reactions of Bis(pinacolato)diboron, 1,3-Enynes, and Aldehydes Catalyzed by an Easily Accessible Bisphosphine–Cu Complex. J. Am. Chem. Soc 2014, 136, 11304–11307. [PubMed: 25089917]

(32). Yang Y; Perry IB; Lu G; Liu P; Buchwald SL Copper-catalyzed asymmetric addition of olefin-derived nucleophiles to ketones. Science 2016, 353, 144–150. [PubMed: 27284169]

(33). Li C; Liu RY; Jesikiewicz LT; Yang Y; Liu P; Buchwald SL CuH-Catalyzed Enantioselective Ketone Allylation with 1,3-Dienes: Scope, Mechanism, and Applications. J. Am. Chem. Soc 2019, 141, 5062–5070. [PubMed: 30817137]

(34). Li C; Shin K; Liu RY; Buchwald SL Engaging Aldehydes in CuH-Catalyzed Reductive Coupling Reactions: Stereoselective Allylation with Unactivated 1,3–Diene Pronucleophiles. Angew. Chem., Int. Ed 2019, 58, 17074–17080.

(35). Liu RY; Zhou Y; Yang Y; Buchwald SL Enantioselective Allylation Using Allene, a Petroleum Cracking Byproduct. J. Am. Chem. Soc 2019, 141, 2251–2256. [PubMed: 30685967]

(36). Tsai EY; Liu RY; Yang Y; Buchwald SL A Regio- and Enantioselective CuH–Catalyzed Ketone Allylation with Terminal Allenes. J. Am. Chem. Soc 2018, 140, 2007–2011. [PubMed: 29376366]

(37). Lee M; Nguyen M; Brandt C; Kaminsky W; Lalic G. Catalytic Hydroalkylation of Allenes. Angew. Chem., Int. Ed 2017, 56, 15703–15707.

(38). Zhang Z; Bera S; Fan C; Hu X. Streamlined Alkylation via Nickel-Hydride-Catalyzed Hydrocarbonation of Alkenes. J. Am. Chem. Soc 2022, 144, 7015–7029. [PubMed: 35413202]

(39). Chen Y. Recent Advances in Methylation: A Guide for Selecting Methylation Reagents. Chem. Eur. J 2019, 25, 3405–3439. [PubMed: 30328642]

(40). Sulikowski GA; Sulikowski MM Iodomethane. In Encyclopedia of Reagents for Organic Synthesis; Wiley: Hoboken, 2005.

(41). Lewis ES; Vanderpool SH Reactivity in methyl transfer reactions. 2. Leaving group effect on rates with substituted thiophenoxides. J. Am. Chem. Soc 1978, 100, 6421–6424.

(42). Finkelstein H. Preparation of Organic Iodides from the Corresponding Bromides and Chlorides. Ber. Dtsch. Chem. Ger 1910, 43, 1528–1532.

(43). Miller JA; Nunn MJ Synthesis of alkyl iodides. J. Chem. Soc., Perkin Trans 1976, 416–420.

(44). Barnett CJ; Wilson TM; Wendel SR; Winningham MJ; Deeter JB Asymmetric Synthesis of Lometrexol ((6R)-5,10-Dideaza-5,6,7,8-tetrahydrofolic Acid). J. Org. Chem 1994, 59, 7038–7045.

(45). Xi Y; Hartwig JF Mechanistic Studies of Copper-Catalyzed Asymmetric Hydroboration of Alkenes. J. Am. Chem. Soc 2017, 139, 12758–12772.

(46). For computational study of enantioinduction in hydrocupration, see: Yang Y; Shi S–L; Niu D; Liu P; Buchwald SL Catalytic asymmetric hydroamination of unactivated internal olefins to aliphatic amines. Science 2015, 349, 62–66. [PubMed: 26138973]

(47). Griffin TR; Cook DB; Haynes A; Pearson JM; Monti D; Morris GE Theoretical and Experimental Evidence for SN2 Transition States in Oxidative Addition of Methyl Iodide to cis-[M(CO)2I2]− (M = Rh, Ir). J.Am. Chem. Soc 1996, 118, 3029–3030.

(48). Mori S; Nakamura E; Morokuma K. Mechanism of S_N2 Alkylation Reactions of Lithium Organocuprate Clusters with Alkyl Halides and Epoxides. Solvent Effects, BF_3 Effects, and Trans-Diaxial Epoxide Opening. J. Am. Chem. Soc 2000, 122, 7294–7307.

(49). Nakamura E; Mori S; Morokuma K. Theoretical Studies on S_N2-Reaction of MeBr with $Me_2CuLi{\cdot}LiCl$. Solvent and Cluster Effects on Oxidative Addition/Reductive Elimination Pathway. J. Am. Chem. Soc 1998, 120, 8273–8274.

(50). In the absence of iodide anion, the methylation using MeOTs is expected to be slower than epimerization. At a lower iodide concentration (e.g., entries 13 and 14, Table 1), due to the low steady state concentration of MeI, methylation with MeI may become slower than benzylcopper epimerization, leading to lower product enantioselectivity.

(51). Fang C; Fantin M; Pan X; de Fiebre K; Coote ML; Matyjaszewski K; Liu P. Mechanistically Guided Predictive Models for Ligand and Initiator Effects in Copper-Catalyzed Atom Transfer Radical Polymerization (Cu-ATRP). J. Am. Chem. Soc 2019, 141, 7486–7497. [PubMed: 30977644]

(52). Saveant JM Dissociative electron transfer. New tests of the theory in the electrochemical and homogeneous reduction of alkyl halides. J.Am. Chem. Soc 1992, 114, 10595–10602.

(53). Cardinale A; Isse AA; Gennaro A; Robert M; Savéant J-M Dissociative Electron Transfer to Haloacetonitriles. An Example of the Dependency of In-Cage Ion-Radical Interactions upon the Leaving Group. J. Am. Chem. Soc 2002, 124, 13533–13539. [PubMed: 12418908]

(54). Several other radical–mediated pathways were considered and were found to be less favorable. See SI, Schemes S3–S5.

(55). Mukaiyama T; Hayashi H; Miwa T; Narasaka K. A New and Effective Asymmetric Synthesis of 3-Phenylalkanals. Chem. Lett 1982, 11, 1637–1640.

(56). Li L; Zhao S; Joshi–Pangu A; Diane M; Biscoe MR Stereospecific Pd-Catalyzed Cross-Coupling Reactions of Secondary Alkylboron Nucleophiles and Aryl Chlorides. J. Am. Chem. Soc 2014, 136, 14027–14030.

(57). Burke MD; Crouch I; Lehmann J; Palazzolo A; Simons C. Stereoretentive Cross-Coupling of Boronic Acids. US2018/305381, 2018.

(58). Rossi D; Urbano M; Pedrali A; Serra M; Zampieri D; Mamolo MG; Laggner C; Zanette C; Florio C; Schepmann D; Wuensch B; Azzolina O; Collina S. Design, synthesis and SAR analysis of novel selective σ1 ligands (Part 2). Bioorg. Med. Chem 2010, 18, 1204–1212. [PubMed: 20045339]

(59). Collina S; Loddo G; Urbano M; Linati L; Callegari A; Ortuso F; Alcaro S; Laggner C; Langer T; Prezzavento O; Ronsisvalle G; Azzolina O. Design, synthesis, and SAR analysis of novel selective σ_1 ligands. Bioorg. Med. Chem 2007, 15, 771–783. [PubMed: 17088069]

(60). Nemeth EF; Wagenen BCV; Balandrin MF; Delmar EG; Moe ST Calcium receptor-active arylalkyl amines. EP1466888, 2004.

(61). Rossi D; Pedrali A; Urbano M; Gaggeri R; Serra M; Fernández L; Fernández M; Caballero J; Ronsisvalle S; Prezzavento O; Schepmann D; Wuensch B; Peviani M; Curti D; Azzolina O; Collina S. Identification of a potent and selective σ1 receptor agonist potentiating NGF-induced neurite outgrowth in PC12 cells. Bioorg. Med. Chem 2011, 19, 6210–6224. [PubMed: 21967807]

(62). Guo J; Hart AC; Macor JE; Mertzman ME; Pitts WJ; Spergel SH; Watterson SH; Andappan Murugaiah Subbaiah M; Chen J; Dzierba CD; Luo G; Shi J; Sit S-Y Amino-triazolopyridines as kinase inhibitors. US10913738, 2021.

(63). Nikam SS; Scott IL; Sherer BA; Wise LD Bicyclic cyclohexylamines and their use as nmda receptor antagonists. US2003/236252, 2003.

(64). Mallams AK; Dasmahapatra B; Neustadt BR; Demma M; Vaccaro HA Quinazoline derivatives useful in cancer treatment. US2007/15774, 2007.

(65). Potts R; Chen T; Rankovic Z; Min J; Lin W; Yang SW; Mayasundari A. Substituted 4-(3-aminoprop-1-yl)aminoquinoline analogs as modelators of melanoma-associated antigen 11 ubiquitin ligase. WO2022/15974, 2022.

(66). Skerlj RT; Bourque EM; Ray S; Lansbury PT Substituted benzimidazole carboxamides and their use in the treatment of medical disorders. WO2021/55591, 2021.

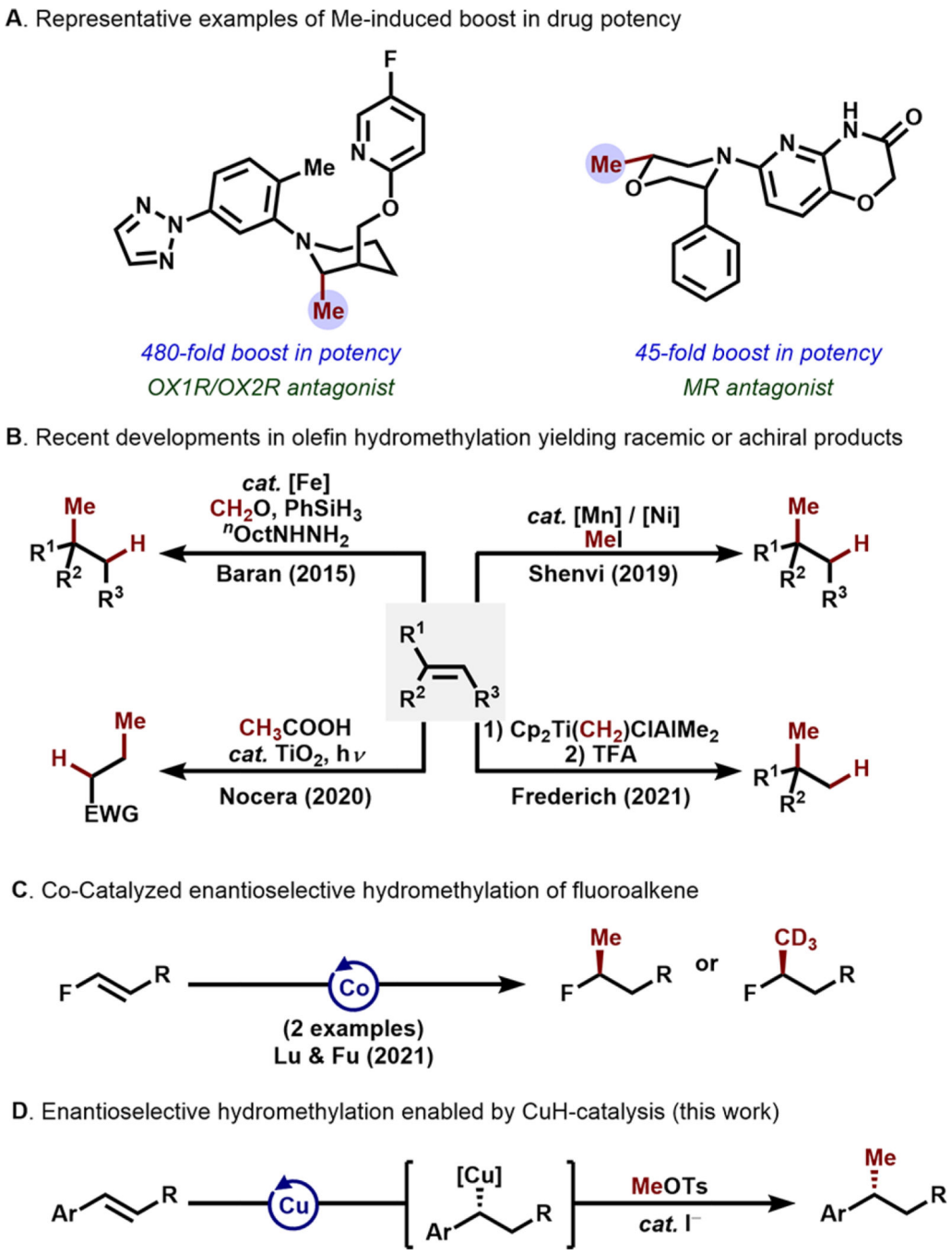

Figure 1.

(A) Representative examples of drug potency increase resulting from the incorporation of a methyl group. (B) Recently reported synthetic protocols for olefin hydromethylation. (C) Co-catalyzed asymmetric hydromethylation of fluoroalkene precursors. (D) Asymmetric olefin hydromethylation using CuH-catalyst supported by chiral bisphosphine ligands.

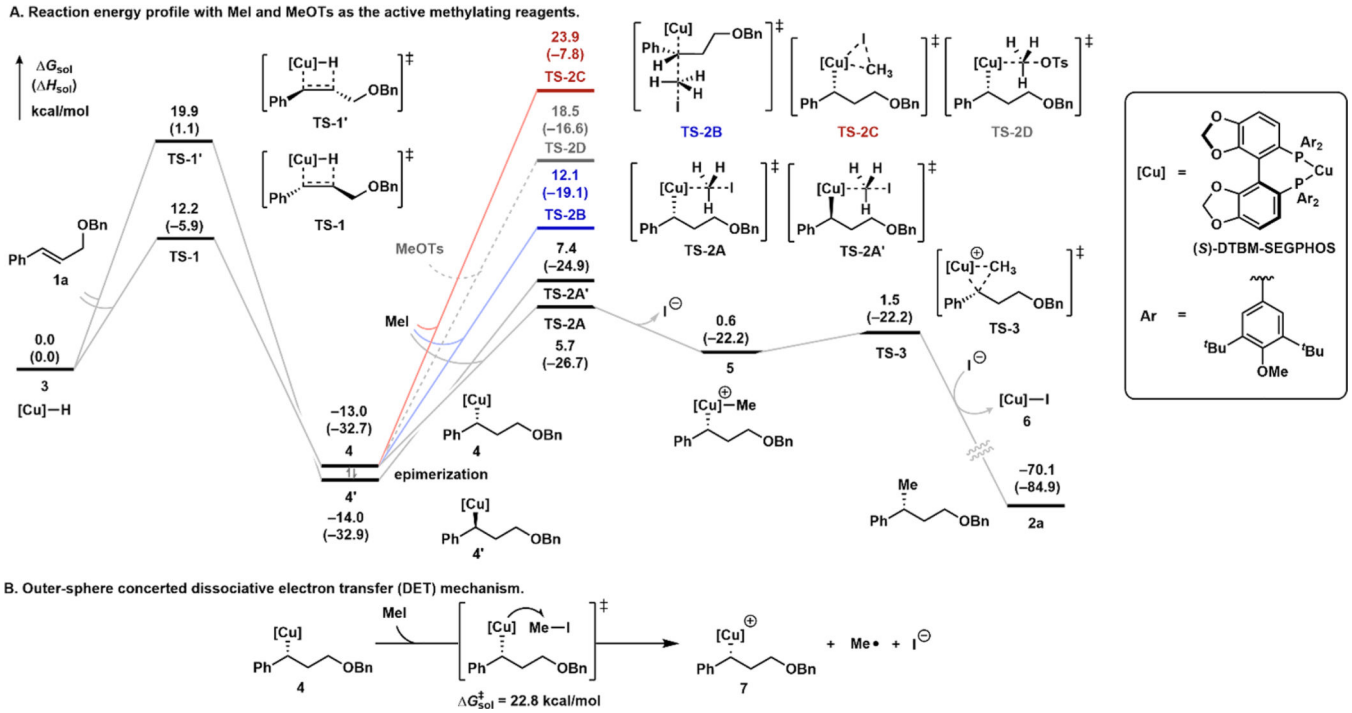

Figure 2.

Computed reaction energy profile (kcal/mol) of the Cu-catalyzed asymmetric hydromethylation.

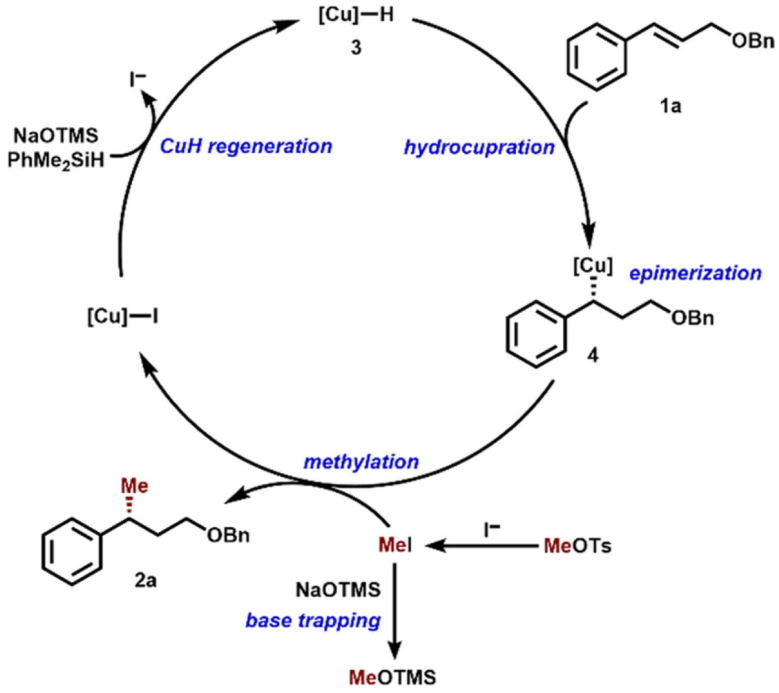

Scheme 1. Proposed Catalytic Cycle

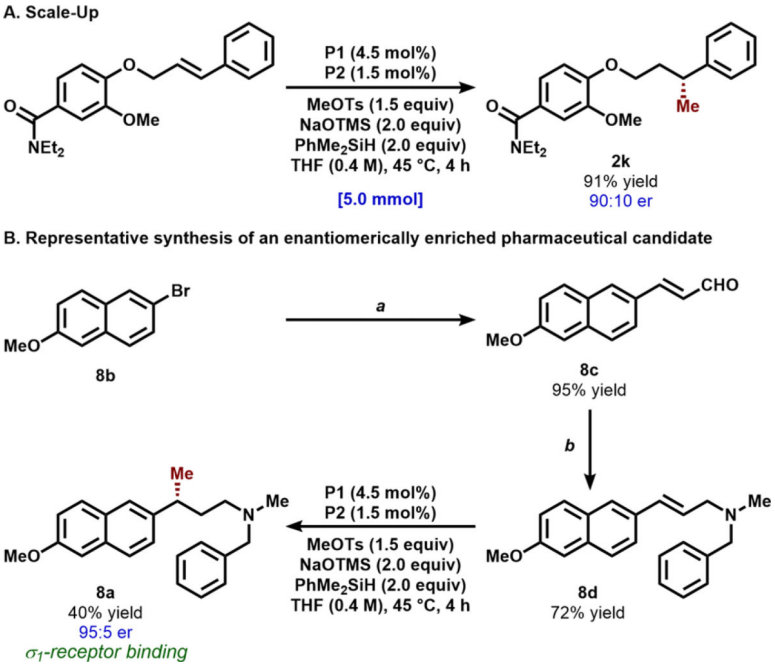

Scheme 2. Application of the CuH-Catalyzed Asymmetric Hydromethylation Reaction

[a]Reaction conditions: 1,1-diethoxyethene (3.0 equiv), $Pd(OAc)_2$ (20.0 mol %), KCl (1.0 equiv), K_2CO_3 (1.5 equiv), ($^nBu_4N$)(OAc) (2.0 equiv), DMF, 90 °C, 16 h. [b]Reaction conditions: (1) *N*-methylbenzylamine (4.0 equiv), H_2SO_4 (5 mol %), DCM, 25 °C, 2 h; (2) $NaBH_4$ (2.0 equiv), DCM, 25 °C, 6 h.

Table 1.

Optimization of the Enantioselective Hydromethylation of (*E*)-(3-(Benzyloxy)prop-1-en-1-yl)benzene (1a) Employing MeOTs as the Methyl Source[a]

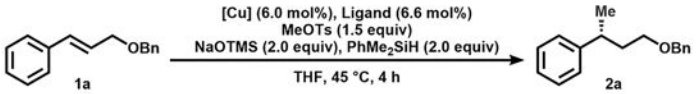

entry	catalyst mixture	yield 2a (%)	er (2a)
1	CuOAc + **L1**	46	37:63
2	CuOAc + **L2**	35	45:55
3	CuOAc + **L3**	<5	-
4	CuOAc + **L4**	55	42:58
5	CuOAc + **L5**	59	64:36
6	CuCl + **L5**	69	81:19
7	CuBr + **L5**	67	73:27
8	CuI + **L5**	76	99:1
9	**P1**	78	99:1
10[b]	**P1** + MeI	47	>99.5:0.5
11[c]	**P1** + MeI	59	99:1
12[d]	**P1** + **P2**	80	95:5
13[e]	**P1** + **P2**	84	79:21
14[f]	**P1** + **P2**	81	75:25

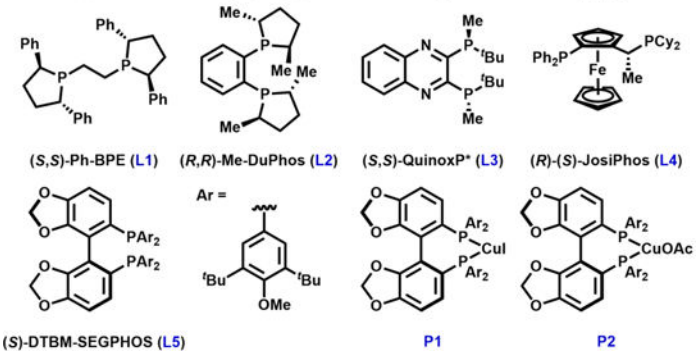

[a]Reaction conditions: 0.20 mmol of (*E*)-(3-(benzyloxy)prop-1-en-1-yl)benzene (**1a**, 1.0 equiv), 0.30 mmol of MeOTs (1.5 equiv), 0.40 mmol of sodium trimethylsilanolate (NaOTMS, 2.0 equiv), 0.40 mmol of $PhMe_2SiH$ (2.0 equiv), specified catalyst mixture, and THF (0.4 M); reaction yields were determined by ^1H NMR spectroscopy of the crude reaction mixture using 1,1,2,2-tetrachloroethane as an internal standard (see SI for details). Enantiomeric ratio (er) of **2a** was determined by chiral supercritical fluid chromatography (SFC).

[b]A catalyst mixture of **P1** (6.0 mol %) and MeI (6.0 mol %) was employed; a significant amount of **1a** (43%) was observed in the product mixture.

[c]A catalyst mixture of **P1** (6.0 mol %) and MeI (3.0 mol %) was employed.

[d]A catalyst mixture of **P1** (4.5 mol %) and **P2** (1.5 mol %) was employed.

[e]A catalyst mixture of **P1** (3.0 mol %) and **P2** (3.0 mol %) was employed.

[f]A catalyst mixture of **P1** (1.5 mol %) and **P2** (4.5 mol %) was employed.

J Am Chem Soc. Author manuscript; available in PMC 2023 September 14.

Table 2.

Substrate Scope of the Enantioselective Hydromethylation Reaction[a]

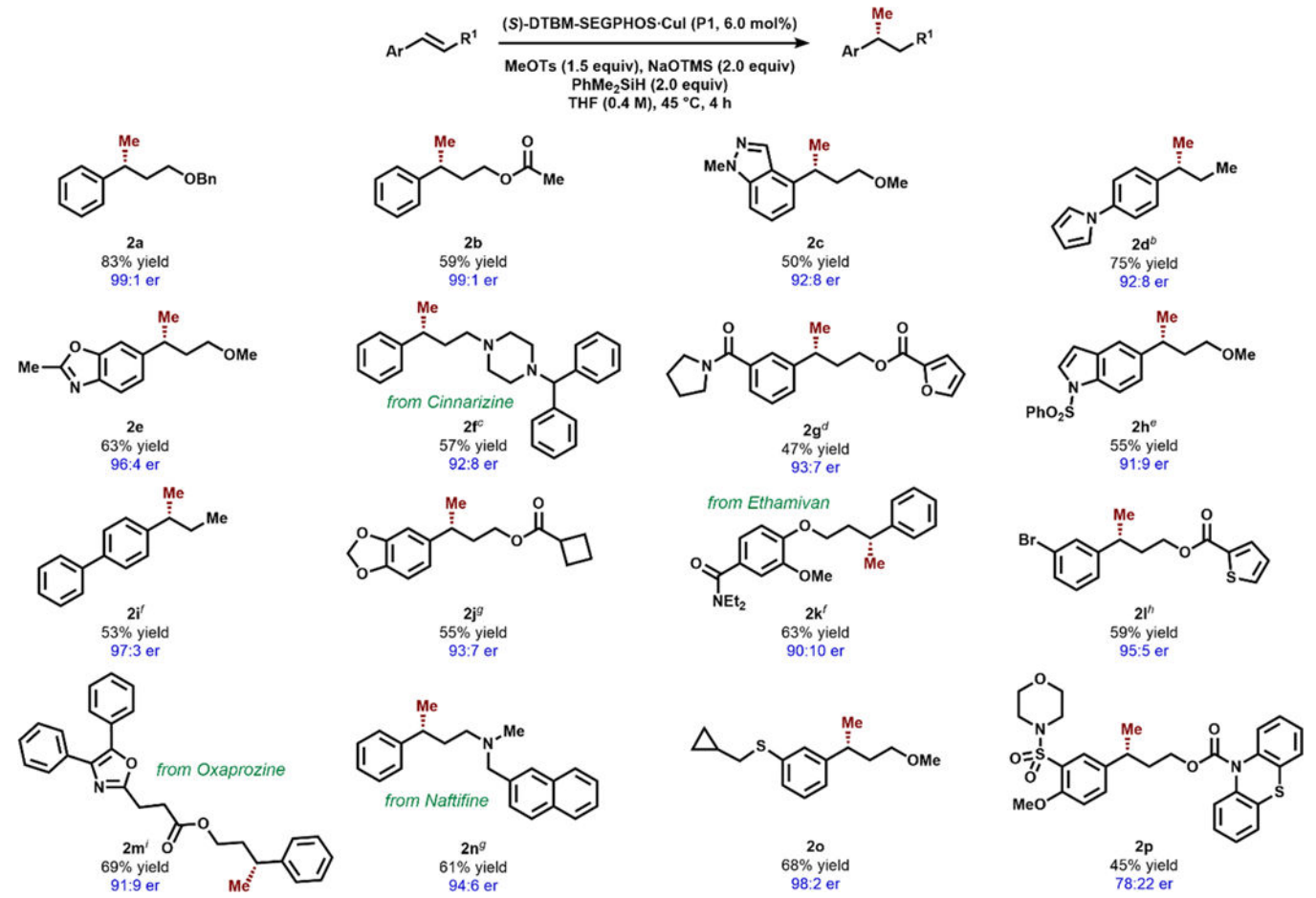

[a]All yields represent the average of two isolated yields using 0.50 mmol of olefin substrate. Enantiomeric ratio (er) was determined by chiral SFC. Precatalyst **P1** (6.0 mol %) was employed unless otherwise noted.

[b]Olefin precursor used as a 9:1 mixture of *E/Z*-isomers; MeOTs was added as a THF stock solution (1.9 M) with 2.0 μL/min addition rate.

[c] MeOTs was added as a THF stock solution (1.9 M) with 8.0 μL/min addition rate.

[d] A catalyst mixture of **P1** (6.0 mol %) and MeI (6.0 mol %) was employed.

[e] A catalyst mixture of **P1** (1.5 mol %) and **P2** (4.5 mol %) was employed.

[f] A catalyst mixture of **P1** (4.5 mol %) and **P2** (1.5 mol %) was employed.

[g] A catalyst mixture of **P1** (3.0 mol %) and **P2** (3.0 mol %) was employed.

[h] A catalyst mixture of **P1** (6.0 mol %) and MeI (30.0 mol %) was employed.

[i] NaOTMS was added as a THF stock solution (1.4 M) with 3.4 μL/min addition rate.